ACS OMEGA

Open Access

http://pubs.acs.org/journal/acsodf

Article

Theoretical Insights into High-T_c Superconductivity of Structurally Ordered $YThH_{18}$: A First-Principles Study

Abdul Ghaffar,* Peng Song, Ryo Maezono, and Kenta Hongo*

Cite This: *ACS Omega* 2024, 9, 49470−49479

Read Online

ACCESS | Metrics & More | Article Recommendations | Supporting Information

ABSTRACT: There has been a marked increase in interest in high-temperature superconductors over the past few years, sparked by their potential to revolutionize multiple fields, including energy generation and transportation. A particularly promising avenue of exploration has emerged in the form of ternary superhydrides, compounds composed of hydrogen along with two other rare-earth elements. Our investigation focuses on the search for Y−Th−H ternary compounds; employing an evolutionary search methodology complemented by electron−phonon calculations reveals a stable superhydride, $P\bar{6}m2$-$YThH_{18}$, capable of exhibiting a critical temperature (T_c) as high as 222 K at 200 GPa along a few low-T_c novel hydrides. Our analysis explores the possibility of alloyed structure formation from the disordered condition of Th-doped YH_9 and establishes that the $P\bar{6}m2$-$YThH_{18}$ is indeed a structurally ordered structure. This opens up an exciting avenue for research on multinary superhydrides, which could facilitate experimental synthesis and provides potential implications for high-temperature superconductivity research.

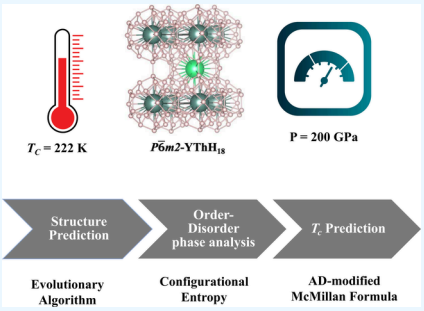

INTRODUCTION

Wigner and Huntington[1] *theoretically* predicted hydrogen to be metallic above 400 GPa and exhibit superconductivity, but such extreme pressures are *experimentally* unreachable even today. In 2004, Ashcroft[2] argued that the incorporation of other metallic elements into the hydrogen system could significantly reduce the transition pressure. This realization prompted investigations into the possibility of high-temperature (high-T_c) superconductivity in metal hydrides, leading to the discovery of high-T_c superconductors, H_3S ($T_c \sim 203$ K at $P = 150$ GPa),[3] YH_{10} (with $T_c > 300$ K at $P \sim 250$ GPa),[4] and LaH_{10} ($T_c \sim 280$ K at $P \sim 200$ GPa).[4−7] Note that these discoveries were initially predicted using an evolutionary algorithm coupled with *ab initio* enthalpy calculations, followed by experimental confirmations.[3,6−8] Recently, several binary hydrides have actually synthesized,[6,7,9−12] which, in turn, have sparked extensive theoretical works into nearly all possible binary hydrides.[13−15]

Recently, a promising avenue has emerged in the field of hydride superconductors through the combination of binary hydrides to form ternary hydrides for their potential to allow for more prototypical superhydrides due to expanding combinatorial space in ternary composition.[16] This development has led to the discovery of high-T_c ternary hydrides,[17−34] some of which have the potential to exhibit higher T_c values at lower P compared to their binary counterparts. For example, Semenok et al.[33] demonstrated experimentally that the unstable binary hydrides such as YH_{10} and LaH_6 in their pure forms may be stabilized into combined ternary hydrides at a relatively lower P. Additionally, the synthesis of the La−Ce−H-based ternary hydride $(La, Ce)H_9$[29] has demonstrated a substantial increase in T_c by 50−80 K, compared to binary CeH_9. This enhancement was attributed to the doping effect of La within the Ce lattice, changing the electronic structure and Fermi surface topology and therefore increasing T_c. Similarly, it has been found experimentally and theoretically that the $(La, Ce)H_{9,10}$ ternary hydrides are superior to their parent binaries.[30] Currently, significant efforts are being directed toward discovering high-T_c superconductivity in hydrides at more moderate or ambient pressure conditions. In this vein, recent trends, reporting superconducting temperatures above 100 K at pressures below 100 GPa, suggest that ternary hydrides could offer a promising route to achieving this goal.[20,27,35,36] Unlike the binary hydrides, however, an exhaustive exploration of ternary (or more) hydrogen-rich hydrides seem impossible because their exploration space gets expanded combinatorially. Although the expanded space increases the probability of finding novel high-T_c hydrides, it also becomes a bottleneck to screen potential thermodynamically stable and high-T_c hydrides even for ternary phases. Thus, the selection of two binaries for ternary candidates usually relies on heuristic strategies: (i) thermodynamically stable and potentially high-T_c binary compounds[37] and (ii) their similarity in electronegativity and atomic size of metals in

Received: August 5, 2024
Revised: October 31, 2024
Accepted: November 6, 2024
Published: December 1, 2024

binary hydrides.[38,39] In this context, we have explored new high-T_c superconductors within the Y−Th−H ternary hydrides employing the genetic algorithm combined with *ab initio* simulations. We discovered that a hydrogen-rich ternary $P\bar{6}m2$-$YThH_{18}$, exhibits a high T_c value of up to 222 K at 200 GPa, alongside two low-T_c hydrides, which can be interpreted as a a consequence of combining the recently synthesized $P6_3/mmc$-YH_9 (~243 at 201 K)[11] and $P6_3/mmc$-ThH_9 (146 K at 179 GPa)[9] systems.

Even if the selection of the two binary hydrides successfully predict a high-T_c ternary hydride candidate, (iii) the third issue generally emerges for ternary (or more complex) hydrogen-rich hydrides, i.e., the structural degree of freedom of two (or more) different metal arrangements. It is widely recognized that elements sharing similar properties such as atomic radii, electronegativity, and electronic configuration typically exhibit a higher propensity for disordered substitutional alloy formation due to its higher configurational entropy.[40−43] In this vein, recent works[43−46] suggest that multiple predicted ternary phases could have more stable, disordered counterparts. This seems to hold even for our Y−Th−H systems because Y and Th atoms have similar physical characteristics (electronegativities of 1.3 and 1.22 on the Pauling scale, respectively, and identical atomic radii of 1.80 Å). This is generally important in multicomponent/high-entropy compounds at higher temperatures.[47,48] Even for multicomponent compounds at higher temperatures, however, ordered structures overcome disordered ones owing to their overwhelming enthalpies arising from their interactions.[49] The present study investigates the order−disorder-competition in the predicted high-T_c ternary phase ($P\bar{6}m2$-$YThH_{18}$), considering the configurational entropy in mixing the Y−H and Th−H building blocks.

The paper begins with computational details explaining our structure search, T_c evaluations, and structural modeling for investigating the order−disorder competition. The result section exhibits the outcomes of new phases predicted by the evolutionary algorithms, their convex-hull phase diagram analysis taking into account configurational entropy effects, superconducting properties, including the electron−phonon interaction. We then discuss how the method/results can provide a basis for predicting and investigating the superconducting property. Finally, we wrap up with the conclusion and acknowledgment sections.

COMPUTATIONAL DETAILS

This study aimed to investigate the existence of stable ternary hydrides with the stoichiometry $(YH_n)_x(ThH_n)_y$, where x and y are positive integers, and n = 4, 6, 9. Note that binary hydrides involving Yttrium (YH_3, YH_6, YH_9)[11,12,50] and Thorium (ThH_4, ThH_6, ThH_{10})[9,51,52] have already demonstrated excellent high-T_c properties. This suggests a strong potential for the formation of stable ternary hydrides through the combination of Y and Th binary systems. Candidate structures for the $(YH_n)_x(ThH_n)_y$ stoichiometry were explored using the variable-composition evolutionary algorithm implemented in the USPEX (Universal Structure Predictor: Evolutionary Xtallography)[53,54] software; the USPEX generated 400 random structures for the given stoichiometry; the evolutionary algorithm was applied to 100 randomly selected structures from the 400 generated structures, and these structures were allowed to evolve with 40% heredity, 40% randomness, 10% soft mutation, and 10% transmutation in every subsequent generation. The search was set to terminate after 20 generations if no new viable candidate structure was detected.

During the structural search, electronic total energies at a given pressure were computed at the level of density functional theory (DFT) with the GGA-PBE exchange-correlation functional.[55] Applied pressures were greater than 100 GPa up to 300 GPa, as both parent binaries are stabilized above 150 GPa. The calculations were conducted using the Vienna Ab-initio Simulation Package (VASP)[56] with projector augmented wave (PAW)[57] scheme. A plane-wave basis set cutoff energy of 600 eV was used, and the Brillouin zone was sampled with a k-point resolution of $2\pi \times 0.03$ Å^{-1}. Full geometry optimization and enthalpy evaluation were performed for all candidate structures at the GGA-PBE level of theory, resulting in the convex-hull diagram used to obtain thermodynamically stable structures. The criteria for the convergence of the self-consistent field (SCF) and maximum force were set to 0.1 meV/atom. The structures were visualized using the VESTA 3 package.[58] We performed first-principles phonon and electron−phonon coupling (EPC) calculations as implemented in the QUANTUM ESPRESSO (QE)[59] package with a PAW pseudopotential[57] at the GGA-PBE level. An energy cutoff of 90 and 700 Ry were employed for wave function and charge density, respectively. The q-point mesh in the Brillouin zone was set to 4 × 4 × 4, and the k-point mesh for the integral of the EPC constant and T_c was set to 16 × 16 × 16.

We applied both (1) the McMillan[60] and (2) the Allen-Dynes (AD) modified McMillan formulas[61] to evaluate T_c only for phases predicted as being stable thermodynamically and dynamically:

(1) The McMillan formula for the T_c value is given as

$$T_c \simeq \frac{\omega_D}{1.45} \exp\left(-\frac{1.04(1+\lambda)}{\lambda - \mu^*(1+0.62\lambda)}\right) \quad (1)$$

where ω_D and μ^* are respectively the Debye frequency and effective Coulomb pseudopotential that is taken as both 0.1 and 0.13 for hydrides. The electron−phonon coupling (EPC) constant (λ) is computed by

$$\lambda = 2\int \frac{\alpha^2F(\omega)}{\omega} d\omega \quad (2)$$

where the electron−phonon spectral function, $\alpha^2F(\omega)$, is given as

$$\alpha^2F(\omega) = \frac{1}{2\pi N(\varepsilon_F)} \sum_{q\nu} \delta(\omega - \omega_{q\nu}) \frac{\gamma_{q\nu}}{\hbar\omega_{q\nu}} \quad (3)$$

where $N(\varepsilon_F)$ represents the density of states at the Fermi level, while $\gamma_{q\nu}$ represents the phonon line width, $\omega_{q\nu}$ is the phonon frequency for wave vector $\mathbf{q}$ and mode ν, and $\hbar$ is the reduced Planck's constant.

(2) The AD modified McMillan formulas is given as

https://doi.org/10.1021/acsomega.4c07199
ACS Omega 2024, 9, 49470−49479

Table 1. Two Computed T_c Values at Certain Pressures for Newly Predicted Phases, along with Relevant Parameters (Electron−Phonon Coupling Constant, λ, Logarithmic Average Frequency, ω_{log}, and Root Mean Squared Phonon Frequency $\bar{\omega}_2$)[a]

System	P [GPa]	λ	$\bar{\omega}_2$	ω_{log} [K]	T_c(McM) μ^* (0.1−0.13)	T_c(AD) μ^* (0.1−0.13)
$P\bar{6}m2$-$YThH_{18}$	200	2.54	27.84	1041.5	173−164	222−205
$P4/mmm$-$YThH_8$	200	0.50	39.97	1351.4	16−10	17−10
$P4/mmm$-$YThH_8$	300	0.41	43.53	1317.4	6−3	6−3
$I4/mmm$-Y_2ThH_{12}	200	0.60	37.42	1169.4	26−18	27−19
$I4/mmm$-Y_2ThH_{12}	300	0.49	42.87	1356.8	16−9	16−10

[a]McM and AD stand for McMillan and AD-modified McMillan formulas, respectively. For each formula, the listed T_c values, separated by a dash, correspond to $\mu^* = 0.10-0.13$.

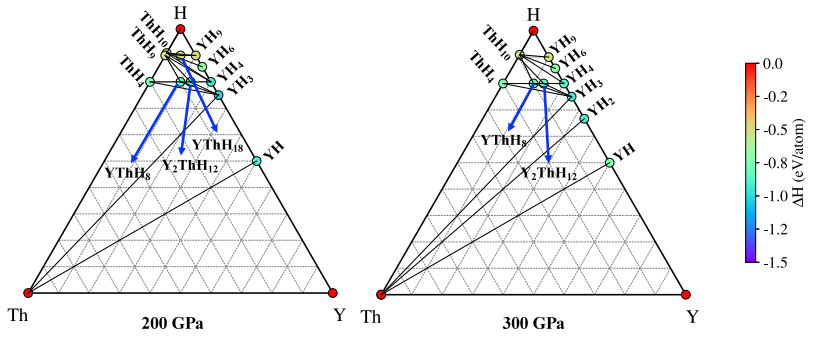

Figure 1. Ternary convex hull diagram of the Y−Th−H system at 200 and 300 GPa obtained using Pymatgen's phase analysis module.[65] Only the stable phases are shown. Black lines connecting the ternaries indicate the shortest synthesis pathways. Out of three stable compositions $YThH_8$, Y_2ThH_{12}, and $YThH_{18}$ was observed at 200 GPa; the $YThH_{18}$ phase disappeared at 300 GPa.

$$T_c = \frac{f_1 f_2 \omega_{log}}{1.2} \exp\left(-\frac{1.04(1+\lambda)}{\lambda - \mu^*(1+0.62\lambda)}\right)$$

$$f_1 = \left(1 + \left(\frac{\lambda}{2.46(1+3.8\mu^*)}\right)^{3/2}\right)^{1/3}$$

$$f_2 = \left(1 + \frac{\lambda^2\left(\frac{\bar{\omega}_2}{\omega_{log}} - 1\right)}{\lambda^2 + \left[1.82(1+6.3\mu^*)\left(\frac{\bar{\omega}_2}{\omega_{log}}\right)\right]^2}\right) \quad (4)$$

where f_1 and f_2 are $\lambda/\mu^*/\omega_{log}/\bar{\omega}_2$-dependent parameters; the logarithmic average frequency (ω_{log}) and the mean square frequency ($\bar{\omega}_2$) are expressed in terms of phonon frequency (ω)

$$\omega_{log} = \exp\left(\frac{\lambda}{2}\int \ln(\omega)\frac{\alpha^2F(\omega)}{\omega}\,d\omega\right) \quad (5)$$

$$\bar{\omega}_2 = \left(\frac{2}{\lambda}\int \alpha^2F(\omega)\omega\,d\omega\right)^{1/2} \quad (6)$$

The present study focuses on the order−disorder competition which arises from the structural degree of freedom for atomic arrangements beyond the binary. To investigate this, a cost-effective structural modeling is critical. To construct the disordered solid solution structure of $Y_xTh_{1-x}H_9$, we employed the special quasi-random structures (SQS) method, as implemented in the sqsgen tool.[62] This method optimizes the Warren-Cowley short-range-order (WC-SRO) parameters[63,64] to ensure a random distribution of Y and Th atoms within the lattice, identifying an optimal disordered configuration. To accommodate the random occupation of Y and Th atoms across 16 lattice sites, we extended the standard unit cell of one of the parent structures ($P6_3/mmc$-YH_9) to a $2 \times 2 \times 2$ supercell, equivalent to 16 $Y_xTh_{1-x}H_9$ formula units. With increasing temperature (T), the configurational entropy of mixing (S_{conf}) can lower the Gibbs free energy (G) as described by $G = H - TS_{conf}$. Equal molar ratios of atoms Y and Th in $YThH_{18}$ configuration suggests the maximum configuration entropy in its disordered form, which can be understood from the following relation

$$\begin{aligned} S_{conf} &\approx k_B \ln(W) \\ &= -R\left(\frac{1}{N}\ln\frac{1}{N} + \cdots + \frac{1}{N}\ln\frac{1}{N}\right) \\ &= R \ln N \end{aligned} \quad (7)$$

where W represents the degree of disorder, k_B is the Boltzmann constant, and R and N are the gas constant and number of elements ($N = 2$ for Y and Th elements) leading to a disordered phase, respectively.

RESULTS

Our newly predicted stable structures for Y−Th−H ternary hydrides and their superconducting properties are given in Figure 2 and in Table 1, respectively. Our key findings reveal three stable structures at $P = 200$ GPa: (1) $P4/mmm$-$YThH_8$, (2) $I4/mmm$-Y_2ThH_{12}, and (3) $P\bar{6}m2$-$YThH_{18}$. Among these, the $P\bar{6}m2$-phase is a high-T_c hydride, exhibiting a transition temperature as high as 222 K at 200 GPa. While $P4/mmm$-$YThH_8$ and $I4/mmm$-Y_2ThH_{12} remain stable up to 300 GPa, they show low superconductivity (below 30 K). Therefore, the

https://doi.org/10.1021/acsomega.4c07199
ACS Omega 2024, 9, 49470−49479

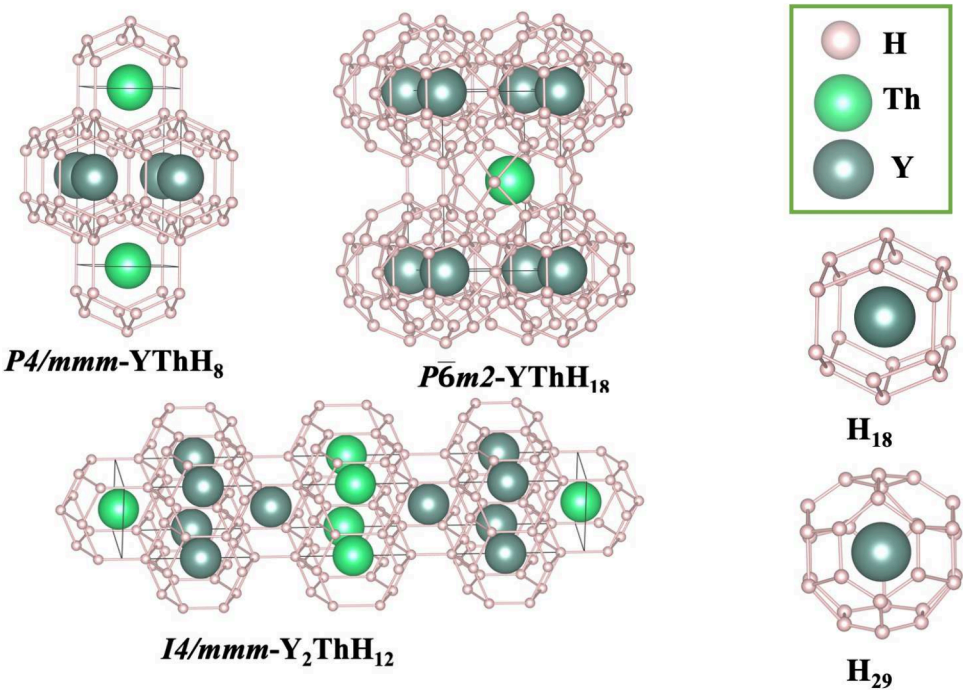

Figure 2. Predicted stable hydrides. $P4/mmm$-$YThH_8$ and $I4/mmm$-Y_2ThH_{12} share H_{18} cages, while $P\bar{6}m2$-$YThH_{18}$ demonstrates H_{29} cages.

subsequent discussion will primarily focus on the promising high-T_c $P\bar{6}m2$-$YThH_{18}$.

Structure prediction and order−disorder competition. Y−H- and Th−H-based binary hydrides, YH_x and ThH_x (where x takes on values of 3, 4, 6, or 9), have already been investigated, some of which exhibit high T_c around $P \sim 200$ GPa. Building on these compounds, we explored various combinations of binaries to form the ternary system Y−Th−H, specifically $(YH_4)_x(ThH_4)_y$, $(YH_6)_x(ThH_6)_y$, and $(YH_9)_x(ThH_9)_y$. The structural stability can be attributed to the dopant element having similar atomic radii and electronic properties, which indicates the stability of the structure against decomposition. Notably, the atomic radii and electronegativity of both elements (Y and Th) are closely matched, providing a strong motivation for our evolutionary search for Y−Th−H systems at pressures ranging from 100 to 300 GPa.

Once we generated novel structures using an evolutionary algorithm for the Y−Th−H chemical system, it was essential to assess their phase stability. Determining the phase stability of ternary hydride involves comparing its energy to that of competing phases. To achieve this, we looked into all the low-energy phases into which the Y−Th−H hydrides could potentially decompose, in addition to their binary (YH_x, ThH_y) and/or elemental constituents (Y, Th, H). To determine the most stable phases in the system, we employed ternary convex hull phase diagram analysis, the results of which are presented in Figure 1. Evidently, at 100 GPa, no stable phases were identified. However, at 200 GPa, the phase diagram analysis revealed three energetically stable structures: $P\bar{6}m2$-$YThH_{18}$, $P4/mmm$-Y_2ThH_{12}, and $I4/mmm$-$YThH_8$. Lattice parameters of all the obtained hydride phases have been summarized in Supporting Information (Table S1). Upon increasing the pressure to 300 GPa, the $P\bar{6}m2$-$YThH_{18}$ phase disappeared from the convex hull diagram. The stable phases exhibit deep hull energies, exceeding −0.53 eV/atom relative to their elemental constituents. This signifies their thermodynamic stability; nevertheless, we can not exclude the possibility of these being disordered alloy structures or metastable phases.

The $YThH_{18}$ composition, characterized by a higher hydrogen content composed of H_{29} cage structures, as shown in Figure 2, indicates its potential as a high-temperature superconductor candidate. Moreover, it is important to consider that this predicted stable structure may undergo phase decomposition with varying pressure. In this line, we analyzed its enthalpies with respect to highly competitive ternary/binary phases identified in our convex hull analysis across a pressure range from 100 to 300 GPa, as depicted in Figure 3. Our aim here is to identify the pressure-dependent phase stability for the highest hydrogen-rich compound against phase transition. There are two critical points corresponding to a stability window ranging from 132 to 222 GPa, suggesting decomposition of $P\bar{6}m2$-$YThH_{18}$ into binary hydrides: (1) at 132 GPa, $P\bar{6}m2$-$YThH_{18} \rightarrow \frac{1}{2}P6_3/mmc$-$YH_9 + \frac{1}{2}P6_3/mmc$-

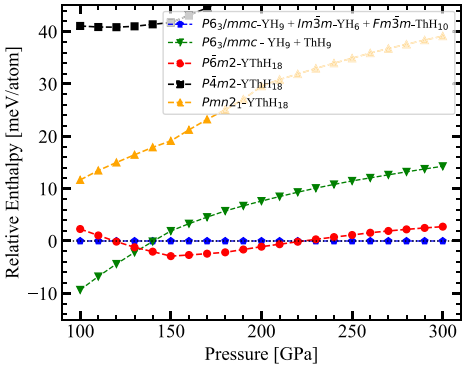

Figure 3. Relative enthalpy of the $P\bar{6}m2$-$YThH_{18}$ phase compared to other competing phases. Labels in the figure denote the compounds contributing toward total enthalpy. This figure underscores the phase stability against decomposition under different pressure conditions.

https://doi.org/10.1021/acsomega.4c07199
ACS Omega 2024, 9, 49470−49479

ThH_9, (2) at 222 GPa, $P\bar{6}m2$-$YThH_{18} \rightarrow \frac{1}{3}P6_3/mmc$-$Y_2H_{18}$ + $\frac{7}{60}Im\bar{3}m$-YH_6 + $\frac{11}{20}Fm\bar{3}m$-ThH_{10}. We anticipate that this hydrogen-rich clathrate hydride could exhibit higher critical temperatures (T_c) due to high-frequency phonon modes mediated by hydrogen and the strong electron−phonon coupling.[3,66,67] The $YThH_{18}$ phase in the $P\bar{6}m2$ symmetry exhibits a hydrogen-to-metal ratio of 9:1, aligning with the expectations of being a promising high-T_c candidate.

The predicted structure can be thought of as a derived structure resulting from one of its parent binaries, for example, Th-substitution on the site of Y in YH_9 binary hydride. Given these observations, we analyzed the possibility that $P\bar{6}m2$-$YThH_{18}$ could be an alloy structure, potentially existing in a disordered form of Th-doped YH_9. To investigate this phenomenon, we analyzed the stability of the ordered phase compared to the disordered structure. We carried out research on the relative stability between the disordered solid solution and the ordered structure in the case of $Y_xTh_{1-x}H_9$. To accomplish this, Gibbs free energy has been calculated in a range of temperatures to account for the increasing configuration entropy (S_{conf}). One can note that the Gibbs free energy follows a decreasing linear trend with temperature given in Figure 4. According to S_{conf} values computed from eq 7 for both ordered and disordered structures, our analysis reveals that the ordered form of the structure $P\bar{6}m2$-$YThH_{18}$ remains stable up to a temperature of 2013 K compared to the disordered structure as demonstrated in Figure 4.

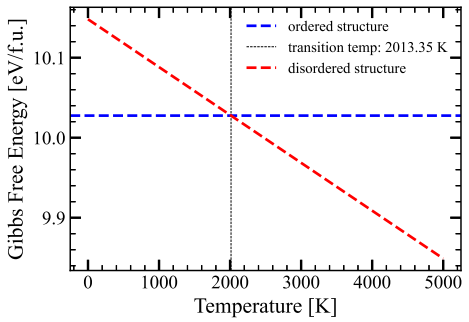

Figure 4. We depict the change in Gibbs free energy with configurational entropy of both the ordered and disordered structures as temperature increases. The vertical black-dotted line represents the transition temperature from the ordered to the disordered structure.

Dynamic stability and Superconductivity. Before delving into the prediction of superconductivity in a compound, it is important to analyze both its dynamic and thermodynamic stability. Thermodynamic stability pertains to the structural stability in the equilibrium configuration of atoms. At the same time, dynamical stability deals with the resilience of a crystal structure when subjected to small atomic vibrations or perturbations. To assess lattice stability under phonon vibrations, we conducted EPC calculations for all the stable hydrides, as depicted in the phonon dispersion relation in Figure 5 and Figure S2, at both 200 and 300 GPa. A consistent trend emerged across all hydrides, where phonon modes could be categorized into two distinct groups: low-frequency modes associated with Th and Y atoms and high-frequency modes composed mainly of H atoms. This observation aligns with the fact that Th and Y are significantly heavier atoms than H, resulting in phonon modes extending up to 8 THz, while H exhibits high-frequency modes ranging from 10 THz to 60 THz.

Specifically, for $P\bar{6}m2$-$YThH_{18}$, the logarithmic frequency (ω_{log}) and the EPC parameter (λ) are 1041.48 K and 2.54, respectively (Figure 5 and Table 1). Notably, the λ value is relatively higher than the reported value for $P6_3/mmc$-ThH_9, which was 1.73 at 150 GPa.[9] Similarly, the λ value is quite high for the $P6_3/mmc$-YH_9 case,[5] reaching 4.42 at 150 GPa. It is essential to note that these λ values may decrease at higher pressures due to phonon hardening.[31] The λ value of 2.54 for $P\bar{6}m2$-$YThH_{18}$, formed from the combination of the two binary hydrides (ThH_9 and YH_9), is reasonable when considering the pressure difference (150 GPa for binaries and 200 GPa for the ternary compound) and the synergistic effect resulting from the combination. The remaining predicted hydrides, specifically $P4/mmm$-$YThH_8$ and $I4/mmm$-Y_2ThH_{12}, at both 200 and 300 GPa, exhibit relatively low λ values, peaking at 0.6 in most cases. The relatively higher λ value for the $YThH_{18}$ structure, compared to other predicted Y−Th−H compositions can be primarily attributed to a significant contribution of H-modes. This is evident from the Eliashberg spectral function ($\alpha^2F(\omega)$), as shown in Figure 5.

We computed the critical temperature (T_c) using both the McMillan formalism (1) and the AD-modified McMillan formula (4), and the results are summarized in Table 1. Typically, a Coulomb pseudopotential (μ^*) ranging from 0.1 to 0.13 is selected for such calculations. As listed in Table 1 the calculation for T_c has been performed on both values. In light of these considerations, we can conclude that $YThH_8$ and Y_2ThH_{12} represent low-T_c hydrides, with typical T_c values of 16 and 26 K at 200 GPa, decreasing by 10 K as the pressure is raised to 300 GPa. In contrast, $P\bar{6}m2$-$YThH_{18}$ demonstrates a significantly high T_c of 222 K when evaluated using the AD formalism, but this value reduces to 173 K when calculated using McMillan's formula. This observation positions $YThH_{18}$ among the ternary superhydrides capable of achieving T_c values exceeding 200 K at pressures not exceeding 200 GPa.

DISCUSSION

The reliability of our genetic algorithm, which is based on the USPEX structure search method to predict structures for the Y−Th−H ternary composition can be assessed by comparing it to recent experimental synthesis efforts guided by structure predictions for Y−H[12] and Th−H[9] binary hydrides. This study assesses phase stability by examining their potential decomposition into various low-order compositions, in addition to evaluating large hull energies and a wide range of pressure stability. These factors collectively increase the likelihood of guiding successful experimental synthesis. It is important to note that the approximations made in predicting critical temperatures (T_c) using the BCS theory-based Eliashberg models (both AD and McMillan formulations) arise from the harmonic approximation. Moreover, a prior prediction[51] using the harmonic approximation with the AD formalism showed good agreement with the synthesis results.[9]

To gain further insights into the high-T_c compounds, it is crucial to quantify the density of states (DOS) derived from hydrogen (H) near the Fermi level, which is a highly sought-after key characteristic of high-T_c hydride compounds.[5] As illustrated in Figure 6 and Figure 5 (also in Figure S1), it is evident that $YThH_{18}$ exhibits the highest H-derived DOS among the compositions considered. This structure also dominates the highest relative DOS attributed to the H

https://doi.org/10.1021/acsomega.4c07199
ACS Omega 2024, 9, 49470−49479

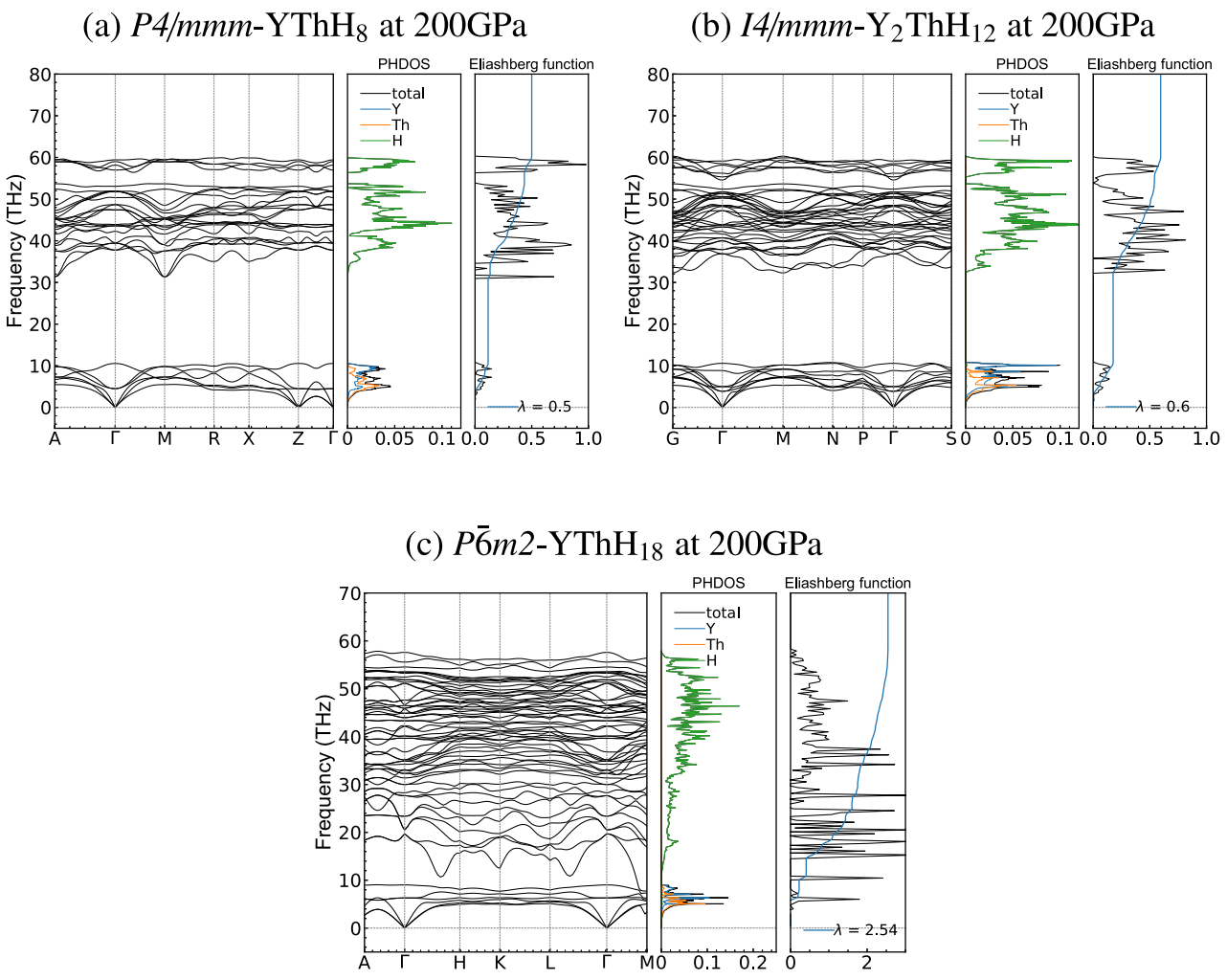

Figure 5. Phonon dispersion, projected phonon density of states (PHDOS), and Eliashberg spectral function $\alpha^2F(\omega)$ associated with the electron−phonon integral ($\lambda(\omega)$) for all the stable compounds. No imaginary modes suggest that all the structures, in addition to their thermodynamic stability are dynamically stable.

element, whereas the other two low-T_c hydrides exhibit a lower H contribution. Apart from the H-derived DOS, the relative hydrogen content in hydride compounds, strongly correlates with superconductivity. For example, in their analysis of over 500 compounds, Wrona et al.[68] found that a lower ratio of the mass of metal atoms to the mass of all hydrogen atoms is a strong predictor of high-T_c compounds. Additionally, our analysis of bonding information reveals that the H−H bond lengths exceed 1.06 Å (for reference, a H_2 molecule has a bond length of approximately 0.74 Å), which is larger than the H−H distance of 0.98 Å in the high-pressure monatomic phase of metallic hydrogen.[69] This suggests the dissociation of H−H molecular bonds. The electron localization function (ELF) values correspond to the lowest H−H bond midpoint exhibiting the highest value of 0.75, indicating that the predicted hydrides imply the presence of weak covalent bonds. It can be seen from Figure 7 that the ELF reduces with increasing bond separation (H−H bonding). Nevertheless, a significant amount of ELF remains at interstitial sites, which, according to chemical template theory,[70] helps explain the stability of hydride compounds. This stabilization favors the formation of an H-sublattice over H_2 units in the presence of metallic sublattices. Further, Bader charge analysis shows that each Y and Th atom loses 1.48 and 1.5 electrons to H atoms, resulting in an average of 0.33 electrons to every H−H bond in the $YThH_{18}$ phase. Additionally, rare earth (RE) elements Y and Th can exhibit oxidation states of +1, +2, and +3 and +1, + 2, + 3, and +4, respectively, which can readily allow for electron donation to the H-sublattice. The electrons acquired by the H−H bonds lead to increased H-derived DOS, which are located in the antibonding σ^*-orbitals since the bonding σ-orbitals, which have lower energies, are already occupied.[71,72] These properties collectively help stabilize the structure and lend an explanation as to why our predicted phase ($P\bar{6}m2$-$YThH_{18}$) can allow for the existence of such a high T_c superconducting property.

In experiments, the use of Y−Th alloy as a precursor for the synthesis of Y−Th−H hydrides under high-temperature and high-pressure conditions can facilitate the formation of disordered alloyed ternary hydrides by readily overcoming the energy barrier posed by the enthalpy of formation.[45] A recent investigation into the La−Th−H-based ternary hydrides by Song et al.[46] demonstrated the possibility of disordered alloy structure formation. This study also suggests that the ordered compositions at ambient conditions gradually stabilize into disordered phases with increasing temperature due to an increase in the configurational entropy of mixing.[43] Along the same line of reasoning, our study involves the calculation of

https://doi.org/10.1021/acsomega.4c07199
ACS Omega 2024, 9, 49470−49479

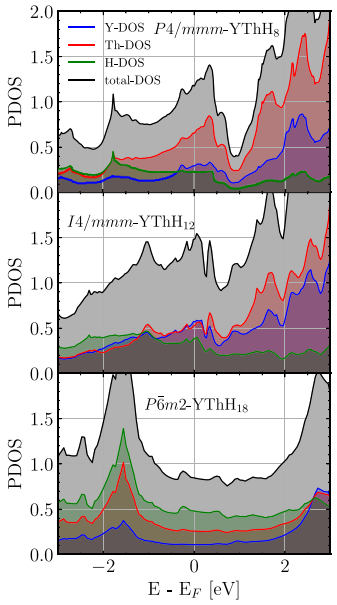

Figure 6. H-derived DOS comparison with different hydrides. The superconducting transition temperature T_c agrees with the observed trend in H-dos.

configurational entropy to predict the transition temperature for stable ordered ternary hydride to disordered alloy composition. The results indicate that the $P\bar{6}m2$-$YThH_{18}$ remains an ordered structure up to a high temperature of over 2000 K. In addition, considering previous studies, where Y-based hydrides[33] generally yield higher T_c than those of La-based,[46] further highlights the significance of this research. In the end, we propose that the experimental synthesis of $P\bar{6}m2$-$YThH_{18}$ can be realized through a usual approach utilizing a diamond anvil cell to produce pressurized hydrides. An alloy of rare-earth metals (Y, Th in the present study) forming the predicted ternary hydrides with NH_3BH_3 as a hydrogen source can be used as precursors. Samples prepared from these can then be loaded into the diamond anvil cell, applying the required pressure, followed by the application of high temperatures up to several hundred degrees Celsius or higher using resistive heating or laser heating. This allows the starting sample to undergo chemical reactions and structural transformations leading to the formation of ternary hydrides. Such synthesis method has been successfully utilized for several recently discovered superconducting hydrides.[26,29,30,33]

CONCLUSION

Our work explores Y−Th−H-based ternary hydrides, a promising avenue for high-temperature superconductivity. By exploiting the chemical similarities of Yttrium and Thorium, and the fact that Y−H and Th−H-based parent binaries have already been synthesized, we identified a novel $YThH_{18}$ superhydride in the $P\bar{6}m2$ phase using a combined evolutionary algorithm and electron−phonon calculations. This material exhibits an impressive critical temperature (T_c) of 222 K at 200 GPa, exceeding many known binary hydride superconductors.[68] Additionally, analysis suggests the ordered structure of $P\bar{6}m2$-$YThH_{18}$ remains stable up to around 2000 K. These findings pave the way for future experimental efforts to synthesize and explore these novel high-temperature superconductors.

ASSOCIATED CONTENT

Data Availability Statement

The data supporting the findings of this study are available at Figshare with the following https://doi.org/10.6084/m9.figshare.27020479.

Supporting Information

The Supporting Information is available free of charge at https://pubs.acs.org/doi/10.1021/acsomega.4c07199.

Crystallographic information on the predicted crystals (Table S1), electronic band structure and density of state plots (Figure S2), phonon dispersion, projected phonon density of states (PHDOS), and Eliashberg spectral function (Figure S2), and project workflow (PDF)

AUTHOR INFORMATION

Corresponding Authors

Abdul Ghaffar − *School of Information Science, JAIST, Nomi 923-1211 Ishikawa, Japan;* Present Address: Materials Science and Technology Division, Oak Ridge National Laboratory, Oak Ridge, Tennessee 37831-2008, United States; orcid.org/0000-0002-4119-0168; Email: mwkabd2101@icloud.com

Kenta Hongo − *Research Center for Advanced Computing Infrastructure, JAIST, Nomi 923-1211 Ishikawa, Japan;*

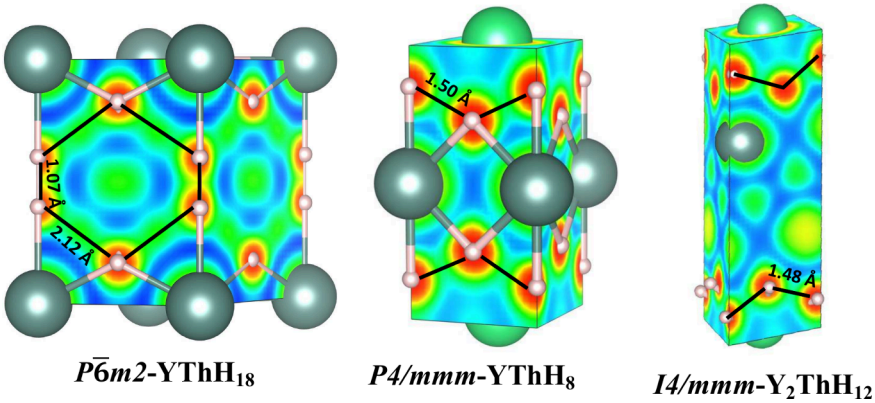

Figure 7. Electron localization function (ELF) presented in all the predicted structures. The lower ELF between H−H bonds indicates a weak covalent bonding. An isosurface value of 0.5 has been used in these plots.

https://doi.org/10.1021/acsomega.4c07199
ACS Omega 2024, 9, 49470−49479

orcid.org/0000-0002-2580-0907;
Email: kenta_hongo@mac.com

Authors

Peng Song − *School of Information Science, JAIST, Nomi 923-1211 Ishikawa, Japan;* Present Address: Institute of Multidisciplinary Research for Advanced Materials, Tohoku University, 2-1-1 Katahira, Aoba-ku, Sendai, Miyagi 980-8577, Japan; orcid.org/0000-0002-9918-2734

Ryo Maezono − *School of Information Science, JAIST, Nomi 923-1211 Ishikawa, Japan;* orcid.org/0000-0002-5875-971X

Complete contact information is available at: https://pubs.acs.org/10.1021/acsomega.4c07199

Notes

The authors declare no competing financial interest.

■ ACKNOWLEDGMENTS

The computations in the present study were performed using the facilities of the Research Center for Advanced Computing Infrastructure (RCACI) at JAIST. A.G. is thankful for the financial support from the MEXT scholarship provided by the Ministry of Education, Culture, Sports, Science, and Technology of Japan. P.S. is grateful for financial support from Grant-in-Aid for JSPS Research Fellow (Grant No. 22J10527). R.M. is grateful for financial support from MEXT-KAKENHI (JP22H05146, JP21K03400), from the Air Force Office of Scientific Research (AFOSR-AOARD/FA2386-17-1-4049; FA2386-19-1-4015), and from JSPS Bilateral Joint Projects (JPJSBP120197714). K.H. is grateful for financial support from MEXT-KAKENHI, Japan (JP19K05029, JP21K03400, JP22H02170, and JP23H04623), and the Air Force Office of Scientific Research, United States (Award Numbers: FA2386-22-1-4065).

■ REFERENCES

(1) Wigner, E.; Huntington, H. B. On the Possibility of a Metallic Modification of Hydrogen. *J. Chem. Phys.* **1935**, *3*, 764−770.
(2) Ashcroft, N. W. Hydrogen Dominant Metallic Alloys: High Temperature Superconductors. *Phys. Rev. Lett.* **2004**, *92*, 187002.
(3) Drozdov, A. P.; Eremets, M. I.; Troyan, I. A.; Ksenofontov, V.; Shylin, S. I. Conventional superconductivity at 203 K at high pressures in the sulfur hydride system. *Nature* **2015**, *525*, 73−76.
(4) Liu, H.; Naumov, I. I.; Hoffmann, R.; Ashcroft, N. W.; Hemley, R. J. Potential high-T_c superconducting lanthanum and yttrium hydrides at high pressure. *Proc. Natl. Acad. Sci. U. S. A.* **2017**, *114*, 6990−6995.
(5) Peng, F.; Sun, Y.; Pickard, C. J.; Needs, R. J.; Wu, Q.; Ma, Y. Hydrogen Clathrate Structures in Rare Earth Hydrides at High Pressures: Possible Route to Room-Temperature Superconductivity. *Phys. Rev. Lett.* **2017**, *119*, 107001.
(6) Drozdov, A. P.; Kong, P. P.; Minkov, V. S.; Besedin, S. P.; Kuzovnikov, M. A.; Mozaffari, S.; Balicas, L.; Balakirev, F. F.; Graf, D. E.; Prakapenka, V. B.; Greenberg, E.; Knyazev, D. A.; Tkacz, M.; Eremets, M. I. Superconductivity at 250K in lanthanum hydride under high pressures. *Nature* **2019**, *569*, 528−531.
(7) Somayazulu, M.; Ahart, M.; Mishra, A. K.; Geballe, Z. M.; Baldini, M.; Meng, Y.; Struzhkin, V. V.; Hemley, R. J. Evidence for Superconductivity above 260K in Lanthanum Superhydride at Megabar Pressures. *Phys. Rev. Lett.* **2019**, *122*, 027001.
(8) Snider, E.; Dasenbrock-Gammon, N.; McBride, R.; Wang, X.; Meyers, N.; Lawler, K. V.; Zurek, E.; Salamat, A.; Dias, R. P. Synthesis of Yttrium Superhydride Superconductor with a Transition Temperature up to 262 K by Catalytic Hydrogenation at High Pressures. *Phys. Rev. Lett.* **2021**, *126*, 117003.
(9) Semenok, D. V.; Kvashnin, A. G.; Ivanova, A. G.; Svitlyk, V.; Fominski, V. Y.; Sadakov, A. V.; Sobolevskiy, O. A.; Pudalov, V. M.; Troyan, I. A.; Oganov, A. R. Superconductivity at 161K in thorium hydride ThH10: Synthesis and properties. *Mater. Today* **2020**, *33*, 36−44.
(10) Chen, W.; Semenok, D.; Huang, X.; Shu, H.; Li, X.; Duan, D.; Cui, T.; Oganov, A. High-Temperature Superconducting Phases in Cerium Superhydride with a Tc up to 115K below a Pressure of 1Megabar. *Phys. Rev. Lett.* **2021**, *127*, 117001.
(11) Kong, P.; Minkov, V. S.; Kuzovnikov, M. A.; Drozdov, A. P.; Besedin, S. P.; Mozaffari, S.; Balicas, L.; Balakirev, F. F.; Prakapenka, V. B.; Chariton, S.; Knyazev, D. A.; Greenberg, E.; Eremets, M. I. Superconductivity up to 243K in the yttrium-hydrogen system under high pressure. *Nat. Commun.* **2021**, *12*, 5075.
(12) Troyan, I. A.; Semenok, D. V.; Kvashnin, A. G.; Sadakov, A. V.; Sobolevskiy, O. A.; Pudalov, V. M.; Ivanova, A. G.; Prakapenka, V. B.; Greenberg, E.; Gavriliuk, A. G.; Lyubutin, I. S.; Struzhkin, V. V.; Bergara, A.; Errea, I.; Bianco, R.; Calandra, M.; Mauri, F.; Monacelli, L.; Akashi, R.; Oganov, A. R. Anomalous High-Temperature Superconductivity in YH6. *Adv. Mater.* **2021**, *33*, 2006832.
(13) Semenok, D. V.; Kruglov, I. A.; Savkin, I. A.; Kvashnin, A. G.; Oganov, A. R. On Distribution of Superconductivity in Metal Hydrides. *Curr. Opin. Solid State Mater. Sci.* **2020**, *24*, No. 100808.
(14) Flores-Livas, J. A.; Boeri, L.; Sanna, A.; Profeta, G.; Arita, R.; Eremets, M. A perspective on conventional high-temperature superconductors at high pressure: Methods and materials. *Phys. Rep.* **2020**, *856*, 1−78.
(15) Gao, G.; Wang, L.; Li, M.; Zhang, J.; Howie, R. T.; Gregoryanz, E.; Struzhkin, V. V.; Wang, L.; Tse, J. S. Superconducting binary hydrides: Theoretical predictions and experimental progresses. *Materials Today Physics* **2021**, *21*, No. 100546.
(16) Flores-Livas, J. A.; Boeri, L.; Sanna, A.; Profeta, G.; Arita, R.; Eremets, M. A perspective on conventional high-temperature superconductors at high pressure: Methods and materials. *Phys. Rep.* **2020**, *856*, 1−78.
(17) Liu, Z.; Hou, W.; Botana, J.; Sun, Y.; Sun, Y.; Yi, W.; Chen, Y. Unexpected Metastable High-Temperature Superconducting Hydride LaCaH12 with an Irregular Cage Structure at High Pressure. *J. Phys. Chem. C* **2023**, *127*, 23870−23878.
(18) Chen, S.; Wang, Y.; Bai, F.; Wu, X.; Wu, X.; Pakhomova, A.; Guo, J.; Huang, X.; Cui, T. Superior Superconducting Properties Realized in Quaternary La-Y-Ce Hydrides at Moderate Pressures. *J. Am. Chem. Soc.* **2024**, *146*, 14105−14113.
(19) Song, X.; Hao, X.; Wei, X.; He, X.-L.; Liu, H.; Ma, L.; Liu, G.; Wang, H.; Niu, J.; Wang, S.; Qi, Y.; Liu, Z.; Hu, W.; Xu, B.; Wang, L.; Gao, G.; Tian, Y. Superconductivity above 105 K in Nonclathrate Ternary Lanthanum Borohydride below Megabar Pressure. *J. Am. Chem. Soc.* **2024**, *146*, 13797−13804.
(20) Wei, X.; Hao, X.; Bergara, A.; Zurek, E.; Liang, X.; Wang, L.; Song, X.; Li, P.; Wang, L.; Gao, G.; Tian, Y. Designing ternary superconducting hydrides with A15-type structure at moderate pressures. *Materials Today Physics* **2023**, *34*, No. 101086.
(21) Gao, K.; Cui, W.; Shi, J.; Durajski, A. P.; Hao, J.; Botti, S.; Marques, M. A. L.; Li, Y. Prediction of high-Tc superconductivity in ternary actinium beryllium hydrides at low pressure. *Phys. Rev. B* **2024**, *109*, 014501.
(22) Sun, W.; Chen, B.; Li, X.; Peng, F.; Hermann, A.; Lu, C. Ternary Na-P-H superconductor under high pressure. *Phys. Rev. B* **2023**, *107*, 214511.
(23) Shutov, G. M.; Semenok, D. V.; Kruglov, I. A.; Oganov, A. R. Ternary superconducting hydrides in the La-Mg-H system. *Materials Today Physics* **2024**, *40*, No. 101300.
(24) Durajski, A. P.; Szcześniak, R. First-Principles Estimation of Low-Pressure Superconductivity in KC2H8 Ternary Hydride. *physica status solidi (RRL)Rapid Research Letters* **2023**, *17*, 2300043.
(25) Qin, K. S.; Song, P.; Hongo, K.; Maezono, R. First-Principles Investigation of Stability and Superconductivity in Ternary Yttrium-

Praseodymium Hydrides under High Pressure. *J. Phys. Chem. C* **2023**, *127*, 21242−21249.
(26) Song, Y.; Bi, J.; Nakamoto, Y.; Shimizu, K.; Liu, H.; Zou, B.; Liu, G.; Wang, H.; Ma, Y. Stoichiometric Ternary Superhydride $LaBeH_8$ as a New Template for High-Temperature Superconductivity at 110K under 80 GPa. *Phys. Rev. Lett.* **2023**, *130*, 266001.
(27) Di Cataldo, S.; Heil, C.; von der Linden, W.; Boeri, L. La BH 8: Towards high-T c low-pressure superconductivity in ternary superhydrides. *Phys. Rev. B* **2021**, *104*, No. L020511.
(28) Semenok, D. V.; Troyan, I. A.; Sadakov, A. V.; Zhou, D.; Galasso, M.; Kvashnin, A. G.; Kruglov, I. A.; Bykov, A. A.; Terent'ev, K. Y.; Cherepahin, A. V.; et al. Effect of paramagnetic impurities on superconductivity in polyhydrides: s-wave order parameter in Nd-doped LaH10. **2022**. DOI: 10.48550/arXiv.2203.06500.
(29) Bi, J.; Nakamoto, Y.; Zhang, P.; Shimizu, K.; Zou, B.; Liu, H.; Zhou, M.; Liu, G.; Wang, H.; Ma, Y. Giant enhancement of superconducting critical temperature in substitutional alloy (La, Ce)H9. *Nat. Commun.* **2022**, *13*, 5952.
(30) Chen, W.; Huang, X.; Semenok, D. V.; Chen, S.; Zhou, D.; Zhang, K.; Oganov, A. R.; Cui, T. Enhancement of superconducting properties in the La-Ce-H system at moderate pressures. *Nat. Commun.* **2023**, *14*, 2660.
(31) Liang, X.; Bergara, A.; Wang, L.; Wen, B.; Zhao, Z.; Zhou, X.-F.; He, J.; Gao, G.; Tian, Y. Potential high-T c superconductivity in CaYH 12 under pressure. *Phys. Rev. B* **2019**, *99*, No. 100505.
(32) Xie, H.; Duan, D.; Shao, Z.; Song, H.; Wang, Y.; Xiao, X.; Li, D.; Tian, F.; Liu, B.; Cui, T. High-temperature superconductivity in ternary clathrate YCaH12 under high pressures. *J. Phys.: Condens. Matter* **2019**, *31*, No. 245404.
(33) Semenok, D. V.; Troyan, I. A.; Ivanova, A. G.; Kvashnin, A. G.; Kruglov, I. A.; Hanfland, M.; Sadakov, A. V.; Sobolevskiy, O. A.; Pervakov, K. S.; Lyubutin, I. S.; Glazyrin, K. V.; Giordano, N.; Karimov, D. N.; Vasiliev, A. L.; Akashi, R.; Pudalov, V. M.; Oganov, A. R. Superconductivity at 253K in lanthanum-yttrium ternary hydrides. *Mater. Today* **2021**, *48*, 18−28.
(34) Song, P.; Hou, Z.; de Castro, P. B.; Nakano, K.; Hongo, K.; Takano, Y.; Maezono, R. High-Tc ternary metal hydrides, YKH12 and LaKH12, discovered by machine learning. 2021. DOI: 10.48550/arXiv.2103.00193.
(35) Vocaturo, R.; Tresca, C.; Ghiringhelli, G.; Profeta, G. Prediction of ambient-pressure superconductivity in ternary hydride PdCuHx. *J. Appl. Phys.* **2022**, *131*, 033903.
(36) Sun, Y.; Sun, S.; Zhong, X.; Liu, H. Prediction for high superconducting ternary hydrides below megabar pressure. *J. Phys.: Condens. Matter* **2022**, *34*, No. 505404.
(37) Bi, J.; Nakamoto, Y.; Shimizu, K.; Zhou, M.; Wang, H.; Liu, G.; Ma, Y. Efficient route to achieve superconductivity improvement via substitutional La-Ce alloy superhydride at high pressure. 2022. DOI: 10.48550/arXiv.2204.04623.
(38) Rahm, M.; Cammi, R.; Ashcroft, N. W.; Hoffmann, R. Squeezing All Elements in the Periodic Table: Electron Configuration and Electronegativity of the Atoms under Compression. *J. Am. Chem. Soc.* **2019**, *141*, 10253−10271.
(39) George, E. P.; Raabe, D.; Ritchie, R. O. High-entropy alloys. *Nature Reviews Materials* **2019**, *4*, 515−534.
(40) Inoue, A.; Ohtera, K.; Masumoto, T. New Amorphous Al-Y, Al-La and Al-Ce Alloys Prepared by Melt Spinning. *Jpn. J. Appl. Phys.* **1988**, *27*, L736.
(41) Solozhenko, V. L.; Kurakevych, O. O.; Andrault, D.; Le Godec, Y.; Mezouar, M. Ultimate Metastable Solubility of Boron in Diamond: Synthesis of Superhard Diamond-like BC_5. *Phys. Rev. Lett.* **2009**, *102*, 015506.
(42) Zhang, M.; Liu, H.; Li, Q.; Gao, B.; Wang, Y.; Li, H.; Chen, C.; Ma, Y. Superhard in BC_3 Cubic Diamond Structure. *Phys. Rev. Lett.* **2015**, *114*, 015502.
(43) Bi, J.; Nakamoto, Y.; Zhang, P.; Wang, Y.; Ma, L.; Wang, Y.; Zou, B.; Shimizu, K.; Liu, H.; Zhou, M.; Wang, H.; Liu, G.; Ma, Y. Stabilization of superconductive La-Y alloy superhydride with Tc above 90K at megabar pressure. *Materials Today Physics* **2022**, *28*, No. 100840.
(44) Wang, T.; Flores-Livas, J. A.; Nomoto, T.; Ma, Y.; Koretsune, T.; Arita, R. Optimal alloying in hydrides: Reaching room-temperature superconductivity in LaH_{10}. *Phys. Rev. B* **2022**, *105*, 174516.
(45) George, E. P.; Raabe, D.; Ritchie, R. O. High-entropy alloys. *Nature Reviews Materials* **2019**, *4*, 515−534.
(46) Song, P.; Durajski, A. P.; Hou, Z.; Ghaffar, A.; Dahule, R.; Szczęśniak, R.; Hongo, K.; Maezono, R. (La,Th)H10: Potential High-Tc (242 K) Superconductors Stabilized Thermodynamically below 200 GPa. *J. Phys. Chem. C* **2024**, *128*, 2656−2665.
(47) Nix, F. C.; Shockley, W. Order-Disorder Transformations in Alloys. *Rev. Mod. Phys.* **1938**, *10*, 1−71.
(48) Zawadzki, P.; Zakutayev, A.; Lany, S. Entropy-Driven Clustering in Tetrahedrally Bonded Multinary Materials. *Physical Review Applied* **2015**, *3*, 034007.
(49) Mizuseki, H.; Sahara, R.; Hongo, K. Order-disorder competition in equiatomic 3d-transition-metal quaternary alloys: phase stability and electronic structure. *Science and Technology of Advanced Materials: Methods* **2023**, *3*, No. 2153632.
(50) Heil, C.; Di Cataldo, S.; Bachelet, G. B.; Boeri, L. Superconductivity in sodalite-like yttrium hydride clathrates. *Phys. Rev. B* **2019**, *99*, No. 220502.
(51) Kvashnin, A. G.; Semenok, D. V.; Kruglov, I. A.; Wrona, I. A.; Oganov, A. R. High-temperature superconductivity in a Th-H system under pressure conditions. *ACS Appl. Mater. Interfaces* **2018**, *10*, 43809−43816.
(52) Yao, S.; Wang, C.; Jeon, H.; Liu, L.; Bok, J. M.; Bang, Y.; Jia, Y.; Cho, J.-H. Origin of the large differences in high-pressure stability and superconductivity between ThH9 and ThH18. 2023. DOI: 10.48550/arXiv.2302.06956.
(53) Glass, C. W.; Oganov, A. R.; Hansen, N. USPEX—Evolutionary crystal structure prediction. *Comput. Phys. Commun.* **2006**, *175*, 713−720.
(54) Oganov, A. R.; Glass, C. W. Crystal structure prediction using ab initio evolutionary techniques: Principles and applications. *J. Chem. Phys.* **2006**, *124*, 244704.
(55) Perdew, J. P.; Burke, K.; Ernzerhof, M. Generalized Gradient Approximation Made Simple. *Phys. Rev. Lett.* **1996**, *77*, 3865−3868.
(56) Kresse, G.; Furthmüller, J. Efficient iterative schemes for ab initio total-energy calculations using a plane-wave basis set. *Phys. Rev. B* **1996**, *54*, 11169−11186.
(57) Blöchl, P. E. Projector augmented-wave method. *Phys. Rev. B* **1994**, *50*, 17953−17979.
(58) Momma, K.; Izumi, F. VESTA3 for three-dimensional visualization of crystal, volumetric and morphology data. *J. Appl. Crystallogr.* **2011**, *44*, 1272−1276.
(59) Giannozzi, P.; Baroni, S.; Bonini, N.; Calandra, M.; Car, R.; Cavazzoni, C.; Ceresoli, D.; Chiarotti, G. L.; Cococcioni, M.; Dabo, I.; Corso, A. D.; de Gironcoli, S.; Fabris, S.; Fratesi, G.; Gebauer, R.; Gerstmann, U.; Gougoussis, C.; Kokalj, A.; Lazzeri, M.; Martin-Samos, L.; Marzari, N.; Mauri, F.; Mazzarello, R.; Paolini, S.; Pasquarello, A.; Paulatto, L.; Sbraccia, C.; Scandolo, S.; Sclauzero, G.; Seitsonen, A. P.; Smogunov, A.; Umari, P.; Wentzcovitch, R. M. QUANTUM ESPRESSO: a modular and open-source software project for quantum simulations of materials. *J. Phys.: Condens. Matter* **2009**, *21*, No. 395502.
(60) McMillan, W. L. Transition Temperature of Strong-Coupled Superconductors. *Phys. Rev.* **1968**, *167*, 331−344.
(61) Allen, P. B.; Dynes, R. Transition temperature of strong-coupled superconductors reanalyzed. *Phys. Rev. B* **1975**, *12*, 905.
(62) Gehringer, D.; Friák, M.; Holec, D. Models of configurationally-complex alloys made simple. *Comput. Phys. Commun.* **2023**, *286*, No. 108664.
(63) Cowley, J. An approximate theory of order in alloys. *Phys. Rev.* **1950**, *77*, 669.
(64) Cowley, J. Short-range order and long-range order parameters. *Phys. Rev.* **1965**, *138*, No. A1384.

https://doi.org/10.1021/acsomega.4c07199
ACS Omega 2024, 9, 49470−49479

(65) Ong, S. P.; Wang, L.; Kang, B.; Ceder, G. Li-Fe-P-O2 Phase Diagram from First Principles Calculations. *Chem. Mater.* **2008**, *20*, 1798−1807.
(66) Mao, W. L.; Mao, H.-k. Hydrogen storage in molecular compounds. *Proc. Natl. Acad. Sci. U. S. A.* **2004**, *101*, 708−710.
(67) Duan, D.; Liu, Y.; Tian, F.; Li, D.; Huang, X.; Zhao, Z.; Yu, H.; Liu, B.; Tian, W.; Cui, T. Pressure-induced metallization of dense (H2S)2H2 with high-Tc superconductivity. *Sci. Rep.* **2014**, *4*, 6968.
(68) Wrona, I. A.; Niegodajew, P.; Durajski, A. P. A recipe for an effective selection of promising candidates for high-temperature superconductors among binary hydrides. *Materials Today Physics* **2024**, *46*, No. 101499.
(69) McMahon, J. M.; Ceperley, D. M. Ground-State Structures of Atomic Metallic Hydrogen. *Phys. Rev. Lett.* **2011**, *106*, 165302.
(70) Sun, Y.; Miao, M. Chemical templates that assemble the metal superhydrides. *Chem.* **2023**, *9*, 443−459.
(71) Wang, H.; Tse, J. S.; Tanaka, K.; Iitaka, T.; Ma, Y. Superconductive sodalite-like clathrate calcium hydride at high pressures. *Proc. Natl. Acad. Sci. U. S. A.* **2012**, *109*, 6463−6466.
(72) Zhang, L.; Wang, Y.; Lv, J.; Ma, Y. Materials discovery at high pressures. *Nature Reviews Materials* **2017**, *2*, 17005.

https://doi.org/10.1021/acsomega.4c07199
ACS Omega 2024, 9, 49470−49479